Binding of Actinomycin D to DNA Oligomers of CXG Trinucleotide Repeats†

Fu-Ming Chen*

Department of Chemistry, Tennessee State University, Nashville, Tennessee 37209-1561

Received August 25, 1997; Revised Manuscript Received December 18, 1997

ABSTRACT: Actinomycin D (ACTD) binding propensities of DNA with CXG trinucleotide repeats were investigated using oligomers of the form d[AT(CXG)$_{n=2-4}$AT] and their corresponding heteroduplexes, where X = A, C, G, or T. These oligonucleotides contain -CXGCXG-, -CXGCXGCXG-, and -CXGCXGCXGCXG- units that can form homoduplexes containing one, two, and three GpC binding sites, respectively, with flanking X/X mismatches. The corresponding heteroduplexes contain these same sites with flanking Watson−Crick base pairs. It was found that oligomers with X = G exhibit weak ACTD affinities whereas those with X ≠ G and $n = 3$ exhibit unusually strong ACTD binding affinities with binding constants ranging from 2.3×10^7 to 3.3×10^7 M^{-1} and binding densities of approximately 1 drug molecule/strand (or 2/duplex). These binding affinities are considerably higher than those of their shorter and longer counterparts and are about 2- and 10-fold stronger than the corresponding CAG·CTG and CGG·CCG heteroduplexes, respectively. The CTG-containing oligomer d[AT(CTG)$_3$AT] stands out as unique in having its ACTD dissociation kinetics being dominated by a strikingly slow process with a characteristic time of 205 min at 20 °C, which is 100-fold slower than d[AT(CAG)$_3$AT], nearly 10-fold slower than the corresponding heteroduplex, and considerably slower than d[AT(CTG)$_2$AT] (63 min) and d[AT(CTG)$_4$AT] (16 min). The faster dissociation rate of the $n = 4$ oligomer compared to its $n = 2$ counterpart is in apparent contrast with the observed 10-fold stronger ACTD binding affinity of the former. It was also found that d[AT(CCG)$_3$AT] exhibits the slowest dissociation rate of the CGG/CCG series, being more than an order of magnitude slower than that of its heteroduplex (τ_{slow} of 43 vs 2 min). The finding that a homoduplex d[AT-CXG-CXG-CXG-AT]$_2$ can bind two ACTD molecules tightly is significant since it was thought unlikely for two consecutive GpC sites separated by a single T/T mismatch to do so.

Actinomycin D (ACTD) is an antitumor antibiotic that contains a 2-aminophenoxazin-3-one chromophore and two cyclic pentapeptide lactones. The biological activity of this drug is believed to be the consequence of its ability to bind to duplex DNA so as to inhibit the DNA-dependent RNA polymerase activities. The DNA binding mode and base sequence specificity of ACTD have been well characterized by X-ray crystallography (*1*−*4*), footprinting (*5*−*13*), and hydrodynamic (*14*) and spectroscopic (*15*−*22*) measurements. The ACTD−DNA complex is formed by the phenoxazinone chromophore of ACTD intercalating into the 5′GpC3′ sequence from the minor groove, with the two cyclic pentapeptide rings anchoring on both sides of the minor groove and covering four base pairs of DNA. The formation of four threonine−guanine hydrogen bonds accounts for the preference of this drug for the 5′GpC3′ step. These essential drug−DNA hydrogen bonds are protected by the cyclic pentapeptides, which effectively shield them from solvent exposure (*4*). The size of the four-base-paired binding site suggests that the binding characteristics of ACTD to the GpC site may be affected by the adjacent flanking base pairs. Indeed, studies with self- as well as non-self-complementary -XGCY-containing decameric duplexes (*23, 24*) have revealed that the binding affinity and dissociation kinetics of this drug are greatly affected by the nature of X and Y bases. For example, ACTD binds strongly to and dissociates very slowly from the -TGCA- site, whereas it binds weakly and dissociates very rapidly from the -GGCC- sequence. Similar adjacent base-pair effects had also been observed by others (*25, 26*). In addition to the observed GpC sequence preference, there have been other reports to indicate that this drug can also bind to some non-GpC sites (*27*−*29*). Of some interests are the observations of ACTD binding to some single-stranded DNA (*30, 31*) and of strong ACTD binding and slow dissociation from the -TGGGT- duplex site (*26, 32*).

Our studies on the effects of adjacent base pairs on the ACTD binding to a GpC site have recently been extended to include flanking base-pair mismatches (*33*). The results indicate that ACTD binds strongly to a GpC site with flanking T/T mismatches and moderately to that with C/C mismatches but weakly to those with G/G or A/A mismatches. The slow component of the ACTD association kinetics at the T/T-mismatched GpC site is slower than those of the self-complementary sequences, whereas that of dissociation is only slightly faster than that of -TGCA- sequence but is decidedly slower than those of -AGCT- and -CGCG- sites and is more than an order of magnitude slower than those with C/C, G/G, and A/A mismatches. These results suggest that the minor-groove environment near the T/T-

† Research supported by Army Medical Research Grant DAMD17-94-J-4474 and a subproject of Minority Biomedical Research Support Grant S06GM0892.

* Telephone (615) 963-5325; Fax (615) 963-5434; E-mail chenf@harpo.tnstate.edu.

S0006-2960(97)02110-7 CCC: $15.00
Published on Web 02/18/1998

mismatched pairs provides favorable interactions with the pentapeptide rings of the drug, whereas the others, especially those of bulkier purine/purine mismatches, result in less favorable interactions.

Lian et al. (*34*) have recently investigated the structural details of the complexes of ACTD with $d(GAAGCTTC)_2$, $d(GATGCATC)_2$, $d(GATGCTTC)_2$, and $d(GAAGCATC)_2$ by nuclear Overhauser effect- (NOE) restrained refinement. It was found that the binding of ACTD to the -$(AGCT)_2$- sequence causes the *N*-methyl group of MeVal of the pentapeptide ring to wedge between the bases at the ApG step, resulting in kinks on both sides of the intercalator site. The van der Waals clashes between adenine base and MeVal-MeN found in -AGCT-, however, become diminished in -TGCA-, making it energetically more favorable. These results provide the structural rationalization for our earlier observed stronger ACTD affinity and slower dissociation kinetics of -TGCA- than those of -AGCT- (*23*). Most interestingly, ACTD was also found to form a very stable complex with $d(GA\text{-}TGCT\text{-}TC)_2$ in which the same methyl group now fits snugly in a cavity at the TpG step created by the T·T mismatched base pair. Such a tight fit apparently provides an increased stability for the binding of ACTD to the -TGCT- sequence. In contrast, ACTD does not stabilize the unstable A·A-mismatched $d(GA\text{-}AGCA\text{-}TC)_2$ duplex to a significant extent. These results have yielded considerable insights and formed the structural basis for our observation that a GpC flanked by T/T mismatches is a tighter and slower-dissociating binding site than the one flanked by A/A (*33*).

In their NMR studies, Lian et al. (*34*) also investigated the ACTD binding with $d(GCTGCTGC)_2$, an octameric duplex containing three consecutive GpC sites separated by single T/T mismatches. The results indicated that this duplex can only bind a maximum of two ACTD molecules with the bound drugs located at the two outer GpC steps. Similar results of two drug molecules binding at the two outer GpC sites, albeit with weaker affinity, were also observed for $d(GCAGCAGC)_2$. The inability of ACTD to bind more than two drug molecules in these three-site systems led them to conclude that the two nearest neighboring GpC sites cannot bind ACTD simultaneously in a sequence such as TGCT-GCT. It was argued that since the outer edges of the peptide rings (i.e., the SarMeVal dipeptide part) of ACTD reach the minor-groove side of the T·T base pairs, there would be severe van der Waals clashes between pentapeptide rings of the two neighboring bound ACTDs. One of the objectives of this report is to investigate the validity of such an assertion.

Effects of base pair mismatches on DNA structures and their ligand interactions are of considerable interest, as they may have relevance in DNA repair, transcription, replication, and activation of damaged genes. In addition, there has recently been intense interests in the study of DNA trinucleotide repeats. This interest stems from the fact that several genetic disorders have been correlated to the dramatic amplification of such repeats in some genes. For example, CGG repeats have been found to be the culprit for the fragile-X syndrome (see ref *35* and references therein), CAG repeats have been shown to be responsible for Huntington's disease and spinobulbar muscular atrophy (*36*, *37*), and CTG repeats have been associated with myotonic dystrophy (*38*, *39*). Although the mechanisms for these trinucleotide expansions are not yet clear, there have been speculations on the roles of unusual DNA conformations such as hairpin formation (*40*−*46*). Our interest in the CXG trinucleotide repeats is further heightened by the fact that heteroduplexes of such repeats contain one or more GpC sites and the formation of homoduplexes from these repeats will result in GpC sites with flanking X/X base mismatches. To understand their ACTD binding characteristics, comparative binding and kinetic studies with oligomers of CXG trinucleotide repeats were carried out via spectroscopic techniques using oligomers of the form $d[AT(CXG)_nAT]$ and their corresponding heteroduplexes, where *n* varies from 2 to 4 and X = any of the four DNA bases. The choice of these oligomers was based on the desire to study the effect of base sequence, chain length, and to avoid possible complications that may arise from ACTD stacking at the terminal G·C base pairs. In particular, we set out to test the assertions that ACTD cannot bind more than two drug molecules in a three-site duplex $(XGCXGCXGCX)_2$ and that the two nearest neighboring GpC sites cannot bind ACTD simultaneously in a sequence such as XGCXGCX (*34*). This report describes our findings and discuss their possible biological implications.

MATERIALS AND METHODS

Synthetic oligonucleotides were purchased from Integrated DNA Technologies, Inc., and used without further purification. All experiments were carried out in 10 mM HEPPS [*N*-(2-hydroxyethyl)piperazine-*N*′-propanesulfonic acid) buffer solutions of pH 8 containing 0.1 M NaCl and 1 mM $MgCl_2$. Concentrations of these oligomers (per nucleotide) were determined by measuring the absorbances at 260 nm after melting, with use of extinction coefficients obtained via nearest-neighbor approximation using mono- and dinucleotide values tabulated in Fasman (*47*). Heteroduplexes were formed by annealing complementary oligomers via heating the equal molar mixtures to 95 °C for 5 min and slowly cooled back to ambient temperature. The extinction coefficients used for drug concentration determination are 24 500 M^{-1} cm^{-1} at 440 nm for ACTD and 23 600 M^{-1} cm^{-1} at 528 nm for 7-amino-ACTD. Absorption spectral measurements were made with a Cary 1E spectrophotometric system. Thermal denaturation experiments were carried out with 1-cm semimicro cells by monitoring absorbances at 275 nm. A heating rate of 0.5 °C/min was maintained by the temperature controller accessory. Spectral titrations were carried out at 20 °C by adding aliquots of DNA stock to the drug solution. Differences of absorbance changes at 427 and 480 nm were used to obtain binding isotherms. Linear least-squares fits of the linear portion of the Scatchard plots with the simple equation $r/m = K_a(n - r)$ were made to estimate the binding parameters, where r is the ratio of bound drug to DNA concentrations, n is the saturation binding density, K_a is the apparent association constant, and m is the free drug concentration. Equations used to calculate the relevant quantities are $C_b = C(\epsilon_f - \epsilon)/(\epsilon_f - \epsilon_b)$, $m = C - C_b$, and $r = C_b/C_{DNA}$, where ϵ_f, ϵ_b, and ϵ are the free, bound, and apparent extinction coefficients of the drug, respectively, whereas C, C_b, and C_{DNA} are total drug, bound drug, and DNA concentrations, respectively. The bound extinction coefficient was obtained via a plot of $1/\epsilon$ vs $1/C_{DNA}$ and an extrapolation to $1/C_{DNA} = 0$. Absorbance kinetic measure-

Table 1: Comparison of Equilibrium Binding and Melting Parameters

oligomer	K_a (μM^{-1})	n (per strand)	t_m^o (°C)	t_m (°C)
d[AT-CAGCAG-AT]	1.1		<20 (b)	34[b], 60(b)
d[AT-CTGCTG-AT]	1.1		<20[b]	43
d[AT-$(CAG)_2$-AT]·d[AT-$(CTG)_2$-AT]	1.8	0.7	40	50
d[AT-CGGCGG-AT]	0.8		<20[b]	30[b], 65[b]
d[AT-CCGCCG-AT]	1.1		<20[b]	33[b], 65[b]
d[AT-$(CGG)_2$-AT]·d[AT-$(CCG)_2$-AT]	0.9		48	55
d[AT-CAGCAGCAG-AT]	32.8	1.2	<20[b]	43[b], 65[b]
d[AT-CTGCTGCTG-AT]	22.6	1.2	27	61
d[AT-$(CAG)_3$-AT]·d[AT-$(CTG)_3$-AT]	11.7	1.2	52	68
d[AT-CGGCGGCGG-AT]	1.3		38[b]	43[b], 65[b]
d[AT-CCGCCGCCG-AT]	26.0	1.2	28[b]	35[b], 68[b]
d[AT-$(CGG)_3$-AT]·d[AT-$(CCG)_3$-AT]	0.8		64	68
d[AT-CAGCAGCAGCAG-AT]	6.2	1.4	46[b]	35[b], 70[b]
d[AT-CTGCTGCTGCTG-AT]	11.8	1.3	51	75
d[AT-$(CAG)_4$-AT]·d[AT-$(CTG)_4$-AT]	8.0	1.8	61	77
d[AT-CGGCGGCGGCGG-AT]	1.4		34[b], 62[b]	38[b], 76[b]
d[AT-CCGCCGCCGCCG-AT]	2.2	1.6	43	35[b], 88[b]
d[AT-$(CGG)_4$-AT]·d[AT-$(CCG)_4$-AT]	1.4		72	76

[a] t_m^o and t_m are the estimated melting temperatures of 40 μM DNA (in nucleotides) solutions containing 0.1 M NaCl in the absence and in the presence of 6 μM ACTD, respectively. [b] The melting profile is too broad to yield accurate melting temperature estimates.

ments were made by using a stirrer accessory with 427 and 453 nm monitorings for the ACTD association and SDS-induced dissociation, respectively. Kinetic rate parameters were extracted using the nonlinear least-squares fit program of GraphPad Prism, whereas binding constants for the multisite binding model were made with the Scientist program of Micromath.

Electrophoretic measurements were made on a Pharmacia Phast system using 20% polyacrylamide gels at 200 V with appropriate pre- and postloading run times at different temperatures. PhastGel native buffer strips containing 0.88 M L-alanine and 0.25 M Tris of pH 8.8 were used, and the gels were developed by silver staining.

RESULTS

ACTD Binds Strongly to d[AT(CXG)$_3$AT], X ≠ G, with a Binding Density of Approximately 1 Drug Molecule/Strand (or 2/Duplex). Comparative ACTD binding studies with oligomers of CXG trinucleotide repeats were carried out via absorbance spectral titrations with oligomers of the form d[AT$(CXG)_{n=2-4}$AT] and their corresponding heteroduplexes. The results are shown as Scatchard plots in Figure 1 and as extracted binding parameters in Table 1. It is immediately apparent from Figure 1 that d[AT$(CGG)_n$AT] (panel E) and their corresponding heteroduplexes (panel D) exhibit weak ACTD binding affinities irrespective of the chain length. In contrast, oligomers with X ≠ G are strongly chain-length dependent, with $n = 3$ exhibiting unusually high ACTD binding affinities that are significantly stronger than that of their $n = 4$ counterparts, and these in turn are considerably higher than those of their corresponding $n = 2$ oligomers (see panels B, C, and F). The extracted binding constants for d[AT$(CXG)_3$AT] with X ≠ G range from 2.3×10^7 to 3.3×10^7 M^{-1} and the binding densities are roughly 1 drug molecule/strand (or 2/duplex) (see Table 1). Interestingly, these binding affinities are about 2-fold stronger than that of the fully hydrogen-bonded d[AT$(CAG)_3$AT]·d[AT-$(CTG)_3$AT] and more than an order of magnitude higher than that of d[AT$(CGG)_3$AT]·d[AT$(CCG)_3$AT]. It should also be noted that the ACTD binding affinities of heteroduplexes containing two, three, and four CAG·CTG repeats (having one, two, and three AGCA·TGCT sites) are about 2×10^6, 12×10^6, and 8×10^6 M^{-1} with binding densities somewhat higher than 1, 2, and 3 drug molecules/duplex, respectively. These binding strengths are approximately 2-, 15-, and 5-fold stronger than their counterparts with CGG·CCG repeats (see Table 1). It is also worthy of note that despite the presence of an additional GpC site and a strong ACTD affinity ($K_a = 1.2 \times 10^7$ M^{-1}), d[AT$(CTG)_4$AT] exhibits a binding density of slightly greater than 2 drug molecules/duplex, which is not greatly different from that of d[AT$(CTG)_3$AT].

Fitting of Binding Isotherms to Multisite Binding Model. In the absence of a linear Scatchard plot, as evident in some plots of Figure 1, the extraction and interpretation of binding parameters from such a plot are not straightforward (see, e.g., ref *48*). Thus, binding isotherms are replotted as r ([bound drugs]/[duplex]) vs m ([free drug]), which are then fitted with a binding model consisting of four consecutive stoichiometric binding constants for the possibility of binding up to 4 drugs per duplex. The relevant equation for this model is (*48*):

$$r = \frac{K_1 m + 2K_1K_2m^2 + 3K_1K_2K_3m^3 + 4K_1K_2K_3K_4m^4}{1 + K_1 m + K_1K_2m^2 + K_1K_2K_3m^3 + K_1K_2K_3K_4m^4}$$

Reasonably good fits are obtained and the extracted binding parameters are summarized in Table 2. Although a good fit does not guarantee the correctness of the extracted parameters, the plausibility of the results is reflected by the exhibited consistent patterns obtained, which are in agreement with those of Scatchard plots.

For the d[AT$(CXG)_2$AT] oligomers, the fits yielded K_3, $K_4 = 0$ and $K_1 \gg K_2$. Except for the considerably weaker binding of d[AT$(CGG)_2$AT], K_1 values are roughly 2.1×10^6 M^{-1}, which is at least an order of magnitude higher than K_2. This is consistent with the presence of one strong binding site -XGCX- in each of these oligomers. Similar binding patterns are found for the heteroduplexes, with the value of K_1 for d[AT$(CAG)_2$AT]·d[AT$(CTG)_2$AT] ($K_1 = 3.9 \times 10^6$ M^{-1}) being somewhat higher than those of its constituent

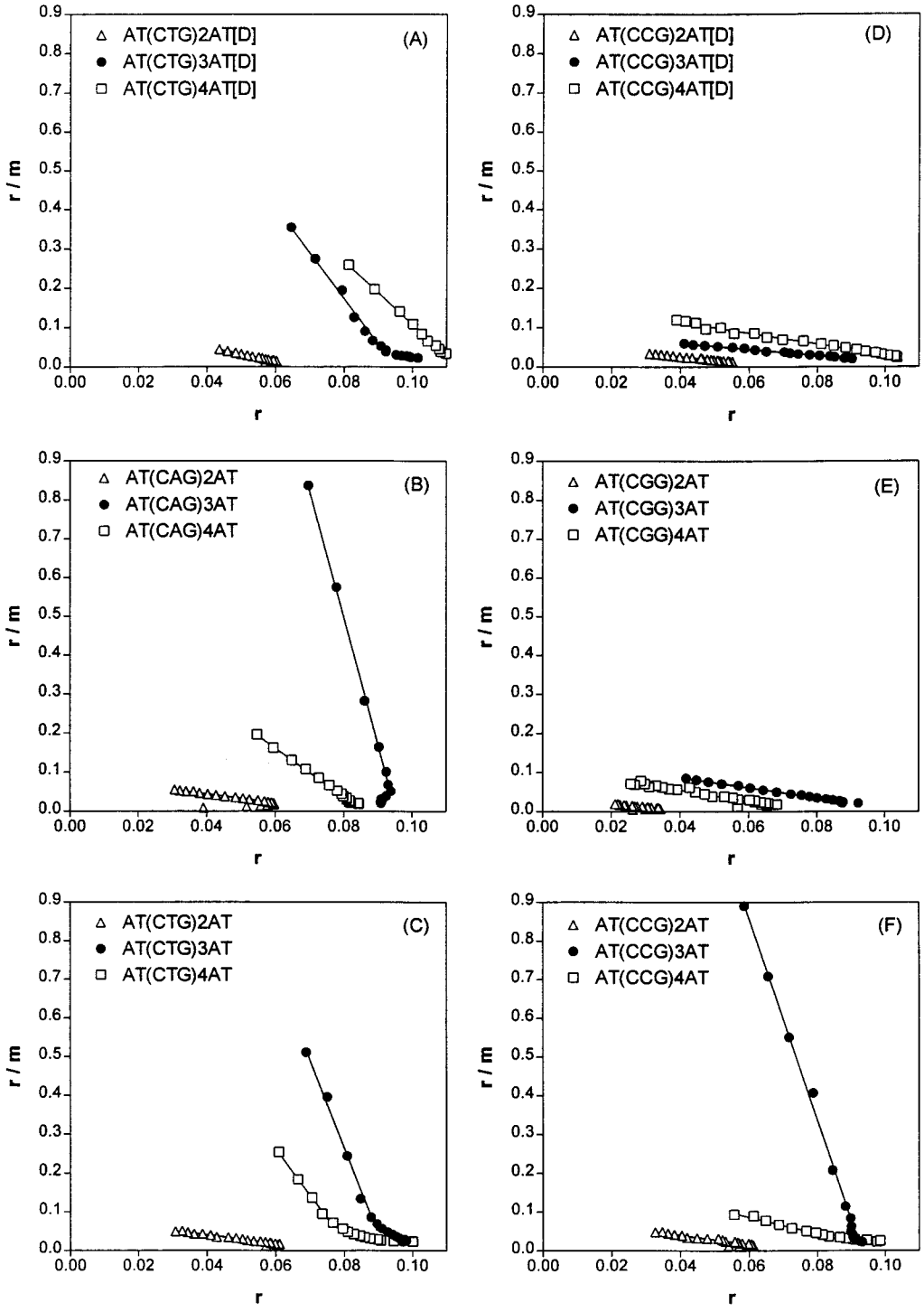

FIGURE 1: Comparison of ACTD equilibrium binding isotherms presented as Scatchard plots for oligomers of CXG trinucleotide repeats at 20 °C. The duplex form is designated as [D] in the figure: d[AT(CAG)$_{n=2-4}$AT]·d[AT(CTG)$_{n=2-4}$AT] (A), d[AT(CAG)$_{n=2-4}$AT] (B), d[AT(CTG)$_{n=2-4}$AT] (C), d[AT(CGG)$_{n=2-4}$AT]·d[AT(CCG)$_{n=2-4}$AT] (D), d[AT(CGG)$_{n=2-4}$AT] (E), and d[AT(CCG)$_{n=2-4}$AT] (F). The absorbance difference between 427 and 480 nm has been used to obtain the binding isotherms. [Bound drug]/[DNA, nucleotide] is designated by *r*, and *m* represents the free drug concentration (micromolar).

oligomers, whereas that of d[AT(CGG)$_2$AT]·d[AT(CCG)$_2$AT] ($K_1 = 1.5 \times 10^6$ M^{-1}) being lower than that of its CCG oligomer. The ordering found for the values of K_1 is consistent with that of binding constants estimated from the Scatchard plots.

Except for the CGG-containing oligomers, which exhibit much weaker binding, the extracted values for the binding constants for the d[AT(CXG)$_3$AT] series exhibit the pattern of $K_4 = 0$ and $K_1 \ll K_2 \gg K_3$, with K_3 being less than 8×10^5 M^{-1} for all oligomers. These results are consistent with the presence of two strong binding sites in these oligomers and the notion of positive cooperative binding for the second drug in these oligomers. In fact, the value of K_1K_2 reflects the overall binding affinity of binding 2 drug molecules to a duplex and ranges from 2.9×10^{14} to 7.8×10^{14} M^{-2} for d[AT(CXG)$_3$AT] with X $\neq$ G. The $(K_1K_2)^{1/2}$ values and their ordering are in agreement with those of ACTD affinities obtained via Scatchard plots. Interestingly, despite the

Table 2: Comparison of Extracted Multisite Stoichiometric Binding Constants[a]

oligomer	K_1 (μM^{-1})	K_2 (μM^{-1})	K_3 (μM^{-1})	K_4 (μM^{-1})
d[AT-CAGCAG-AT]	2.1	0.21	0.00	0.00
d[AT-CTGCTG-AT]	2.1	0.16	0.00	0.00
d[AT-$(CAG)_2$-AT]·d[AT-$(CTG)_2$-AT]	3.9	0.10	0.00	0.00
d[AT-CGGCGG-AT]	<0.4	0.00	0.00	0.00
d[AT-CCGCCG-AT]	2.2	0.14	0.00	0.00
d[AT-$(CGG)_2$-AT]·d[AT-$(CCG)_2$-AT]	1.5	0.08	0.00	0.00
d[AT-CAGCAGCAG-AT]	0.18	4310	0.73	0.00
d[AT-CTGCTGCTG-AT]	0.036	8040	0.37	0.00
d[AT-$(CAG)_3$-AT]·d[AT-$(CTG)_3$-AT]	0.19	840	0.33	0.00
d[AT-CGGCGGCGG-AT]	2.8	1.6	0.23	0.00
d[AT-CCGCCGCCG-AT]	0.21	1830	0.57	0.00
d[AT-$(CGG)_3$-AT]·d[AT-$(CCG)_3$-AT]	2.4	0.80	0.29	0.00
d[AT-CAGCAGCAGCAG-AT]	0.34	160	0.63	0.00
d[AT-CTGCTGCTGCTG-AT]	1.0	55	0.65	0.00
d[AT-$(CAG)_4$-AT]·d[AT-$(CTG)_4$-AT]	0.97	7.1	27	0.36
d[AT-CGGCGGCGGCGG-AT]	3.1	1.3	0.16	0.00
d[AT-CCGCCGCCGCCG-AT]	2.4×10^{-4}	1.4×10^{4}	0.70	0.12
d[AT-$(CGG)_4$-AT]·d[AT-$(CCG)_4$-AT]	28	0.54	2.6	0.19

[a] The equation used for the fits is given in the text.

Table 3: Comparison of 1% SDS-Induced ACTD Dissociation Kinetic Parameters at 20 °C

oligomer	k (%),[a] min^{-1}	k_f (%),[b] min^{-1}	k_s (%),[b] min^{-1}
d[AT-CGG-CGG-AT]	0.6 ± 0.1 (23)	5.7 ± 0.8 (39)	0.33 ± 0.03 (61)
d[AT-CCG-CCG-AT]	2.4 ± 0.2 (56)	3.4 ± 0.1 (78)	0.24 ± 0.04 (22)
d[AT$(CGG)_2$AT]·d[AT$(CCG)_2$AT]	1.16 ± 0.05 (71)	2.3 ± 0.1 (57)	0.49 ± 0.03 (43)
d[AT-CAG-CAG-AT]	1.2 ± 0.1 (73)	1.9 ± 0.1 (73)	0.29 ± 0.04 (27)
d[AT-CTG-CTG-AT]	0.0185 ± 0.0005 (79)	0.29 ± 0.02 (17)	0.0159 ± 0.0002 (83)
d[AT$(CAG)_2$AT]·d[AT$(CTG)_2$AT]	0.0435 ± 0.0004 (98)		
d[AT-CGG-CGG-CGG-AT]	3.6 ± 0.2 (39)	5.5 ± 0.2 (75)	0.7 ± 0.1 (25)
d[AT-CCG-CCG-CCG-AT]	0.037 ± 0.02 (43)	2.7 ± 0.2 (28)	0.023 ± 0.001 (72)
d[AT$(CGG)_3$AT]·d[AT$(CCG)_3$AT]	0.94 ± 0.04 (84)	2.1 ± 0.1 (39)	0.54 ± 0.02 (61)
d[AT-CAG-CAG-CAG-AT]	0.52 ± 0.02 (40)	067 ± 0.05 (73)	0.07 ± 0.11 (27)
d[AT-CTG-CTG-CTG-AT]	0.0071 ± 0.0002 (100)	0.189 ± 0.006 (8)	0.00487 ± 0.00006 (92)
d[AT$(CAG)_3$AT]·d[AT$(CTG)_3$AT]	0.0491 ± 0.0009 (90)	0.41 ± 0.02 (13)	0.0418 ± 0.0004 (87)
d[AT-CGG-CGG-CGG-CGG-AT]	0.95 ± 0.09 (31)	2.3 ± 0.2 (60)	0.20 ± 0.03 (40)
d[AT-CCG-CCG-CCG-CCG-AT]	0.435 ± 0.006 (100)		
d[AT$(CGG)_4$AT]·d[AT$(CCG)_4$AT]	0.78 ± 0.02 (73)	1.14 ± 0.07 (71)	0.25 ± 0.04 (29)
d[AT-CAG-CAG-CAG-CAG-AT]	0.59 ± 0.03 (44)	2.9 ± 0.2 (36)	0.32 ± 0.02 (64)
d[AT-CTG-CTG-CTG-CTG-AT]	0.096 ± 0.007 (62)	0.90 ± 0.05 (34)	0.064 ± 0.001 (66)
d[AT$(CAG)_4$AT]·d[AT$(CTG)_4$AT]	0.0553 ± 0.0006 (90)		

[a] The percentage in this column represents the measurable absorbance change compared to that of the total change. [b] Kinetic parameters extracted via two-exponential fits. The percentages in these columns represent the contributions of the fast (f) and slow (s) kinetic components of the measurable absorbance.

presence of four CXG units, d[AT$(CAG)_4$AT] and d[AT-$(CTG)_4$AT] exhibit binding patterns very similar to those with three CXG units (i.e., $K_4 = 0$ and $K_1 \ll K_2 \gg K_3$). Although four binding constants are needed to achieve good fits for d[AT$(CCG)_4$AT], K_3 and K_4 are considerably smaller than K_2, which in turn is much larger than K_1. These results suggest that only two drug molecules are bound strongly to each of these oligomeric duplexes despite the presence of four CXG (or three XGCX) units. In contrast, the values of the binding constants are in the order of $K_1 < K_2 < K_3 \gg K_4$ for d[AT$(CAG)_4$AT]·d[AT$(CTG)_4$AT], a pattern that is consistent with three drug molecules binding at the three strong binding AGCA·TGCT sites in this duplex exhibiting an overall association binding constant of approximately $K_1K_2K_3 = 1.9 \times 10^{20}$ M^{-3}.

ACTD Dissociates Very Slowly from d[AT(CTG)$_3$AT] with a Rate Nearly an Order of Magnitude Slower Than That of the Corresponding Heteroduplex. SDS-induced dissociation kinetic profiles of ACTD from d[AT$(CXG)_n$AT] and their corresponding heteroduplexes are shown in Figure 2 and the extracted kinetic parameters via one- and two-exponential fits are presented in Table 3. It is immediately apparent from Figure 2 that ACTD dissociates considerably faster from the CGG/CCG series (right panels) than from their CAG/CTG counterparts (left panels; note the 50-fold difference in the time scale). For the latter series, the ACTD dissociation kinetic profiles of d[AT$(CAG)_n$AT] decay significantly faster than those of d[AT$(CTG)_n$AT] and the corresponding heteroduplexes d[AT$(CAG)_n$AT]·d[AT$(CTG)_n$AT]. Most interestingly, the ACTD dissociation kinetics of d[AT-$(CTG)_3$AT], and to a lesser extent those of d[AT$(CTG)_2$AT], are decidedly slower than those of their corresponding heteroduplexes. In fact, the slow dissociation rate of ACTD from d[AT$(CTG)_3$AT] is found to be 0.00487 min^{-1} (or a characteristic time of 205 min), which is 2 orders of magnitude slower than that of the corresponding one with CAG repeats (0.52 min^{-1} or 1.9 min) and nearly an order of magnitude slower than that of the corresponding heteroduplex (0.0418 min^{-1} or 23.9 min). Although the dissociation rates do not vary greatly with chain length for the heteroduplexes,

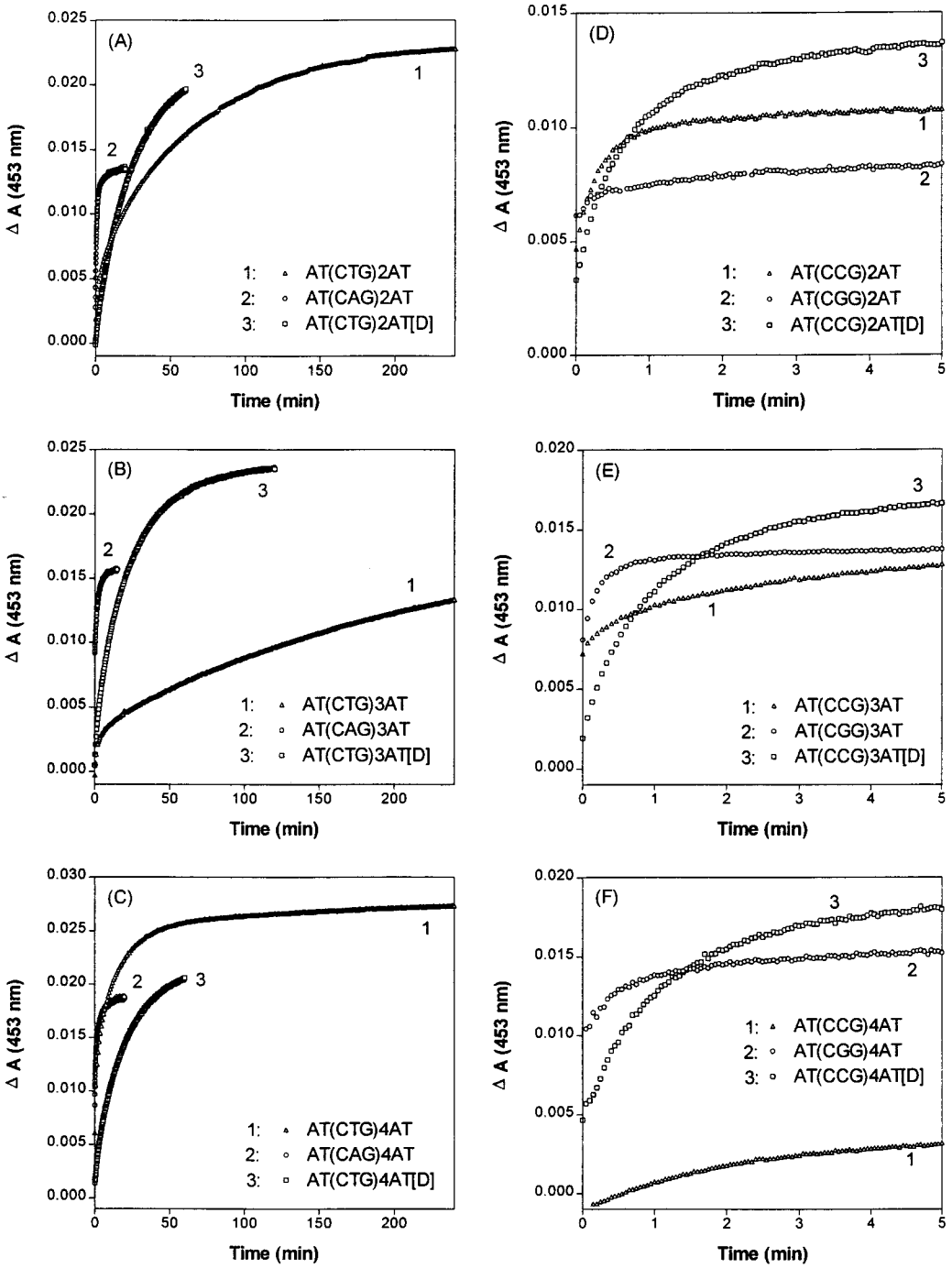

FIGURE 2: Comparison of representative 1% SDS-induced ACTD dissociation kinetic profiles via absorbance monitoring at 20 °C for various oligomers of CXG trinucleotide repeats: d[AT(CAG)$_2$AT]·d[AT(CTG)$_2$AT] and the constituent oligomers (A), d[AT(CAG)$_3$AT]·d[AT(CTG)$_3$AT] and the constituent oligomers (B), d[AT(CAG)$_4$AT]·d[AT(CTG)$_4$AT] and the constituent oligomers (C), d[AT(CGG)$_2$AT]·d[AT(CCG)$_2$AT] and the constituent oligomers (D), d[AT(CGG)$_3$AT]·d[AT(CCG)$_3$AT] and the constituent oligomers (E), d[AT(CGG)$_4$AT]·d[AT(CCG)$_4$AT] and the constituent oligomers (F). The drug dissociation was initiated by adding an appropriate amount of 20% SDS to a solution mixture containing 4 μM ACTD and 80 μM DNA in nucleotide.

they do so strongly for the CTG-containing oligomers. For example, whereas the slowest dissociation component for d[AT(CTG)$_3$AT] exhibits a characteristic time of 205 min, those for d[AT(CTG)$_2$AT] and d[AT(CTG)$_4$AT] are 63 and 15.6 min, respectively. It should be noted that these last two rates cited are in apparent contrast to a 10-fold higher binding affinity ($K_a = 1.2 \times 10^7$ vs 1.1×10^6 M^{-1}) of the four repeats than that of two repeats. Interestingly, d[AT(CCG)$_3$AT] also exhibits the slowest dissociation kinetics in the CGG/CCG series and its slow component is more than an order of magnitude slower than the corresponding heteroduplex (43 vs 1.9 min).

Association kinetic profiles of ACTD binding to d[AT-(CXG)$_n$AT] and their corresponding heteroduplexes have also been measured. The results (not shown) indicate that whereas the heteroduplexes exhibit the largest non-stopped-flow measurable components (ranging from 14% to 43% of the total absorbance changes) and their kinetic profiles can be approximated by single-exponential decays with characteristic lifetimes of 0.3−0.6 min, the constituent oligomers

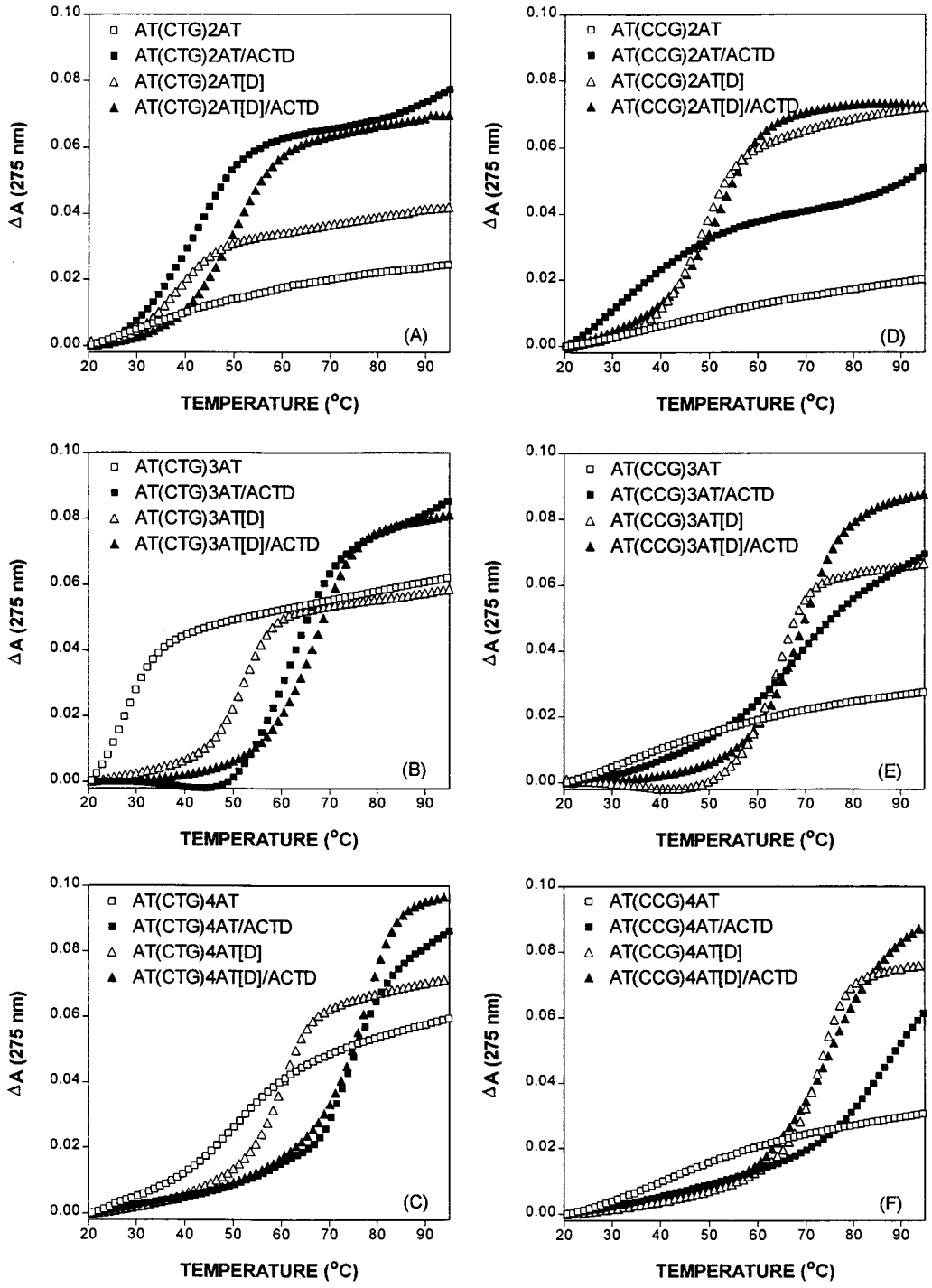

FIGURE 3: Representative thermal melting profiles of various oligomers (40 μM in nucleotide) of CXG trinucleotide repeats in the absence and in the presence of ACTD (6 μM) at pH 8 and 0.1 M NaCl: d[AT(CTG)$_2$AT] and its corresponding heteroduplex (A), d[AT(CTG)$_3$AT] and its corresponding heteroduplex (B), d[AT(CTG)$_4$AT] and its corresponding heteroduplex (C), d[AT(CCG)$_2$AT] and its corresponding heteroduplex (D), d[AT(CCG)$_3$AT] and its corresponding heteroduplex (E), and d[AT(CCG)$_4$AT] and its corresponding heteroduplex(F).

exhibit smaller measurable absorbance changes that require two-exponential fits. Oligomers d[AT(CXG)$_3$AT], X = T and C, are unusual in exhibiting significant contributions from slow association components having characteristic times of about 8 and 5 min, respectively, which are considerably slower than those of their respective longer and shorter counterparts.

Thermal Stabilities of Oligomers with CXG Repeats Are Greatly Enhanced by ACTD Binding. Melting profiles of d[AT(CTG)$_n$AT] (panels A−C) and d[AT(CCG)$_n$AT] (panels D−F) in the absence and in the presence of ACTD are compared with their respective heteroduplexes in Figure 3 and the estimated melting temperatures are included in Table 1. In the absence of ACTD, 40 μM (in nucleotide) d[AT(CAG)$_2$AT]·d[AT(CTG)$_2$AT] at pH 8 with 0.1 M NaCl melts near 40 °C, whereas the melting temperature increases to around 50 °C in the presence of 6 μM ACTD (panel A). In contrast, d[AT(CXG)$_2$AT] alone does not exhibit cooperative melting above 20 °C, suggesting melting temperatures of <20 °C for the homodimeric duplexes. However, a characteristic cooperative melting profile is apparent in the presence of ACTD for d[AT(CTG)$_2$AT], exhibiting a melting

temperature of around 43 °C (panel A). For decamers of X ≠ T, the presence of ACTD results in very diffuse biphasic melting profiles with barely discernible melting temperatures. The dramatic melting temperature increases upon ACTD binding to oligomers with CTG repeats can more clearly be seen with the oligomer of three CTG repeats (see panel B). A cooperative melting near 27 °C is seen for d[AT-$(CTG)_3$AT] but is shifted to 61 °C in the presence of ACTD, a dramatic 34 °C melting temperature increase. In contrast, the melting temperature of d[AT$(CAG)_3$AT]·d[AT$(CTG)_3$AT] only changes from 53 to 68 °C upon ACTD binding. For n = 4, both d[AT$(CAG)_4$AT]·d[AT$(CTG)_4$AT] and d[AT-$(CTG)_3$AT] exhibit melting temperatures of approximately 76 °C in the presence of ACTD, whereas 61 and 51 °C, respectively, are noted in the drug's absence (panel C). Significant ACTD-induced melting temperature increases were also observed for d[AT$(CXG)_n$AT], X ≠ T, but the melting profiles are much broader and biphasic in nature. The much weaker ACTD binding affinities of d[AT-$(CGG)_n$AT]·d[AT$(CCG)_n$AT] are also evidenced by the considerably smaller melting temperature increases upon ACTD binding (see panels D−F).

Our ability to detect a melting temperature above 20 °C for d[AT$(CTG)_3$AT] but not for d[AT$(CAG)_3$AT] is in agreement with the finding of Smith et al. (*43*) indicating that the order in melting temperatures is $[d(CAG)_3]_2$ < $[d(CTG)_3]_2$ ≪ $d(CAG)_3$·$d(CTG)_3$, suggesting that the presence of A·A mismatches in such sequence context has a more profound destabilizing effect than that of T·T mismatches.

DISCUSSION

In summary, ACTD binding studies with oligomers of the form d[AT$(CXG)_{n=2-4}$AT] and their corresponding heteroduplexes, where X = any of the four DNA bases, indicate that the heteroduplexes containing CAG·CTG repeats exhibit higher ACTD binding affinities and more than an order of magnitude slower dissociation kinetics than the CGG·CCG counterparts. Of the constituent oligomers, d[AT$(CGG)_n$AT] oligomers exhibit the weakest ACTD binding affinities and are relatively insensitive to chain length, whereas oligomers with X ≠ G are strongly chain-length-dependent and those with n = 3 exhibit unusually high ACTD binding affinities. The extracted binding constants for d[AT$(CXG)_3$AT] with X = A, C, and T range from 2.3×10^7 to 3.3×10^7 M^{-1} and the binding densities are approximately 1 drug molecule/strand (or 2/duplex). These binding affinities are considerably higher than those of their corresponding longer and shorter counterparts, about 2-fold stronger than that of the fully hydrogen-bonded d[AT$(CAG)_3$AT]·d[AT$(CTG)_3$AT], and more than an order of magnitude higher than that of d[AT$(CGG)_3$AT]·d[AT$(CCG)_3$AT]. Despite the comparable ACTD binding affinities for these X ≠ G oligomers of three repeats, the CTG-containing oligomer d[AT$(CTG)_3$AT] stands out as unique in having its ACTD association kinetic profile exhibiting a significant contribution from a slow component (approximately 8-min lifetime) and its ACTD dissociation kinetics being dominated by a strikingly slow process with a characteristic time of 205 min at 20 °C, which is 100-fold slower than that of d[AT$(CAG)_3$AT] and nearly 10-fold slower than that of the corresponding heteroduplex. In contrast to the heteroduplexes, the dissociation rates of d[AT$(CTG)_n$AT] are found to be strongly chain-length-dependent, as evidenced by the two remaining oligomers in the CTG-repeating series, d[AT$(CTG)_2$AT] and d[AT-$(CTG)_4$AT], exhibiting slow dissociation times of 63 and 15.6 min, respectively. The faster dissociation rate of the n = 4 oligomer appears to be at variance with the observed 10-fold stronger ACTD binding affinity of this oligomer when compared to its n = 2 counterpart. It was also found that d[AT$(CCG)_3$AT] exhibits the slowest dissociation kinetics of the CGG/CCG series and its slow component is more than an order of magnitude slower than that of its heteroduplex (τ_s of 43 vs 1.9 min).

Oligomers of the form d[AT$(CXG)_{n=2-4}$AT] contain -CXGCXG-, -CXGCXGCXG-, and -CXGCXGCXGCXG- units, respectively, which can form homoduplexes consisting of one, two, and three GpC binding sites with flanking X/X mismatches. The finding of unusually strong ACTD binding affinities of d[AT$(CXG)_3$AT], X ≠ G, with two drug molecules bound to a duplex is of particular significance since its homoduplex d[AT-CXG-CXG-CXG-AT]$_2$ is seen to contain two consecutive GpC sites that are separated by an X/X mismatch. Thus, our results suggest that two ACTD molecules can bind tightly to two consecutive GpC sites that are separated by an X/X mismatch, in direct conflict with the assertion of Lian et al. (*34*). It is likely that a duplex with an X/X mismatch is flexible enough to alter the conformation of DNA to accommodate two clashing pentapeptide rings and turn them into van der Waals attractions for snug fit. An outstanding example of two drug molecules binding to two consecutive GpC sites is the formation of a unique 2:1 complex of ACTD to d[ATGCGCAT]$_2$, as studied by NMR (*19*, *20*). It was found that two 1:1 unsymmetric complexes form in unequal proportions at the ratio of 1 ACTD:duplex. At the ratio of 2 ACTD:duplex, however, both COSY and NOESY spectra confirm the formation of a unique 2:1 species with C_2 symmetry. The oligomer remains in a right-handed duplex but undergoes extreme conformational changes both at and adjacent to the binding site. This conformational change widens the minor groove and help alleviate the steric crowding of the ACTD peptides. It is, thus, reasonable to expect that two consecutive GpC sites separated by an X/X mismatch can do likewise with more facility because of the additional spacing introduced by the mismatched base pair.

Formation of a homoduplex by four CXG repeats will result in a duplex, -(CXGCXGCXGCXG)$_2$- consisting of one central and two off-center GpC sites separated by single X/X mismatches. Consequently, results from our d[AT$(CXG)_4$AT] series will in fact be akin to the underlined three-site system investigated by Lian et al. (*34*). Our binding titrations indicate that these oligomers exhibit somewhat smaller ACTD binding affinities than the corresponding oligomers of three repeats but the binding densities remain essentially 1 drug molecule/strand (2/duplex), in agreement with their finding of two drug molecules bound at the two outer sites. The rationale for two instead of three ACTD molecules binding to the three-site systems, d(GCXGCXGC)$_2$, may be that when one of the off-center GpC sites is occupied, a second molecule will prefer the other off-center site instead of the central site to avoid steric hindrance. Once both off-center sites are occupied, the DNA conformational rigidity will be such that an additional binding at the central site will be much more difficult.

It is, however, somewhat puzzling that a nearly 2-fold reduction in the binding affinity and an approximately 10-fold faster ACTD dissociation rate are accompanied by an increase of the CTG repeats from three to four. Similarly, a significant binding reduction is coupled with greater than 10-fold faster dissociation kinetics when the number of CCG repeats is increased from three to four. These results may possibly be rationalized in terms of the absence of close contacts of the intermolecular peptide rings when the two ACTD molecules are bound to the outer GpC sites to result in weaker binding and more facile dissociation processes. The predominance of hairpin conformation in solutions of d[AT(CXG)$_4$AT], especially under the low concentrations used in our optical studies, may have partially contributed to the observed weaker ACTD binding affinities and faster dissociation rates than their $n = 3$ counterparts. A hairpin formation of the $n = 4$ oligomer will result in an X/X-mismatched GpC site on the duplex stem with the central GpC as part of the single-stranded loop, thus, accounting for the observed 1 drug/strand binding densities. Furthermore, the proximity of the duplex binding site to the loop region will likely result in a poorer pentapeptide rings−minor-groove interactions with the consequent more rapid dissociation of ACTD. Our observations of very broad melting profiles in the absence of ACTD and the seemingly biphasic melting curves in the presence of ACTD appear to suggest some contributions from the hairpins. ACTD binding to the hairpin form will be less important for the $n = 3$ oligomers, since the hairpin formation of such oligomers will result in the absence of GpC sites in the duplex stem. Attempts to delineate the relative ACTD binding contributions to dimeric duplex vs hairpin forms were made with electrophoretic experiments using the heteroduplexes as benchmarks (results not shown). The dominance of hairpin species for the $n = 4$ oligomers in the absence of ACTD is readily apparent in the electrophoretic patterns. However, in the presence of the drug, the mobility patterns are characterized by the prominent presence of the ACTD−intermolecular duplex bands and a conspicuous absence of the ACTD−hairpin bands. These results are consistent with the stronger ACTD affinity and/or slower dissociation for the dimeric duplex than for the monomeric hairpin.

Our finding that some of the constituent oligomers, especially those with X = pyrimidine, exhibit stronger ACTD affinities and slower dissociation kinetics than their corresponding heteroduplexes are of significance. One would have anticipated that the dimeric duplex destabilized by the presence of mismatched bases should have resulted in a weaker drug complex that would dissociate very rapidly in the presence of SDS. The anticipated conformational rearrangements and close fits likely account for the observed slow association and dissociation behaviors for d[AT-CXG-CXG-CXG-AT]$_2$. The fact that the X = T and C oligomers provide much slower ACTD dissociation kinetics in their respective series suggests that T/T and C/C mismatches can provide more favorable minor-groove environments for snug fits, likely the consequence of smaller sizes of the pyrimidines. The weaker ACTD binding and faster dissociation kinetics of the corresponding fully hydrogen-bonded heteroduplexes may be the consequence of their diminished conformational flexibility for snugly fitting these pentapeptide rings into the minor groove. The very weak ACTD affinities exhibited by oligomers and their heteroduplexes of CGG repeats most likely are the consequence of the protruding 2-amino groups at the minor groove of the G/G mismatches to result in poor minor-groove interactions with the pentapeptide rings.

The finding that the ACTD binding affinities, the rates of ACTD dissociation, and the melting temperature increases of d[AT(CAG)$_{n=2-4}$AT]·d[AT(CTG)$_{n=2-4}$AT] are respectively higher, slower, and larger than those of d[AT-(CGG)$_{n=2-4}$AT]·d[AT(CCG)$_{n=2-4}$AT] is to be expected. These heteroduplexes consist of one, two, or three units, respectively, of tetranucleotide binding site AGCA·TGCT or GGCG·CGCC. Our earlier studies on the binding specificity of ACTD to duplex tetranucleotide sequences of the form -XGCY- have revealed that the binding affinity and dissociation kinetics of this drug are greatly affected by the nature of X and Y bases (*23*, *24*). In particular, when X = G and/or Y = C, the oligomers exhibit significantly weaker ACTD binding affinities, faster SDS-induced ACTD dissociation rates, and smaller melting temperature increases upon drug binding than the other sequences.

A closer examination of the binding characteristics of oligomers containing a single GpC site with flanking X/X mismatches is of interest. Except for a somewhat smaller value for the X = G oligomer, ACTD binding affinities of d[AT(CXG)$_2$AT] are nearly identical ($K_a = 1.1 \times 10^6$ M^{-1}) which are slightly larger than that of d[AT(CGG)$_2$AT]·d[AT(CCG)$_2$AT] and somewhat smaller than that of d[AT-(CAG)$_2$AT]·d[AT(CTG)$_2$AT] ($K_a = 1.8 \times 10^6$ M^{-1}). Depite their comparable binding affinities, the decamer with X = T exhibits the slowest ACTD association kinetics, more than an order of magnitude slower dissociation kinetics than the other decamers studied, and severalfold slower ACTD dissociation rate than its heteroduplex. Except for the binding order, these results are in general agreement with our earlier studies (*33*) using dodecamers of the form d[ATTA-XGCX-TAAT] and their self-complementary counterparts. The apparent absence of binding preference in the decameric system is at variance with our earlier dodecameric studies, which indicated a binding order of T/T > C/C > G/G, A/A for the mismatched duplexes. These parities may likely be the consequence of differences in chain lengths and flanking sequences. In this connection, it should also be pointed out that despite the earlier finding of weaker ACTD affinity for a GC site with flanking A/A mismatches (*33*, *34*), d[AT(CAG)$_{3-4}$AT] studied here exhibit strong ACTD binding affinities (albeit with rapid dissociation rates) that are comparable to their CTG counterparts. The presence of multiple X/X base-pair mismatches for more facile conformational alterations may have played the key role.

Finally, our finding that the ACTD binding affinities of some constituent oligomers of trinucleotide repeats are stronger than those of their heteroduplexes is consistent with the observation of Lian et al. (*34*) that the annealing propensities of two long DNA oligos, G(CAG)$_{10}$C and G(CTG)$_{10}$, are significantly reduced in the presence of ACTD. Such a phenomenon may have biological relevance since the DNA triplet expansion associated with genetic diseases usually involves a large number of such repeats. It is conceivable that a (CXG)$_n$·(CYG)$_n$ sequence may be in dynamic equilibria with cruciform structures consisting of extended arms composed of (CXG)$_n$ and (CYG)$_n$ homo-

duplexes. The presence of ACTD may, thus, trap these cruciform structures of the $(CXG)_n/(CYG)_n$ sequence by preferentially binding to their stems. Such an interference of equilibrium between a duplex and cruciform structures by a drug or protein can possibly result in serious consequences on the subsequent functions associated with the normal $(CXG)_n \cdot (CYG)_n$ heteroduplexes (*34*).

ACKNOWLEDGMENT

I thank C. Edwards for some technical assistance.

REFERENCES

1. Sobell, H. M., and Jain, S. C. (1972) *J. Mol. Biol. 68*, 21−34.
2. Takusagawa, F., Dabrow, M., Neidle, S., and Berman, H. M. (1982) *Nature 296*, 466−469.
3. Kamitori, S., and Takusagawa, F. (1992) *J. Mol. Biol. 225*, 445−456.
4. Kamitori, S., and Takusagawa, F. (1994) *J. Am. Chem. Soc. 116*, 4154−4165.
5. Lane, M. J., Dabrowiak, J. C., and Vouurrnakis, J. N. (1983) *Proc. Natl. Acad. Sci. U.S.A. 80*, 3260−3264.
6. Scamrov, A. V., and Beabealashvilli, R. Sh. (1983) *FEBS Lett. 164*, 97−101.
7. Van Dyke, M. W., and Dervan, P. B. (1983) *Nucleic Acids Res. 11*, 5555−5567.
8. Van Dyke, M. W., Hertzberg, R. P., and Dervan, P. B. (1983) *Proc. Natl. Acad. Sci. U.S.A. 79*, 5470−5474.
9. Fox, K. R., and Waring, M. J. (1984) *Nucleic Acids Res. 12*, 9271−9285.
10. White, R. J., and Phillips, D. R. (1989) *Biochemistry 28*, 6259−6269.
11. Rehfuss, R., Goodisman, J., and Dabrowiak, J. C. (1990) *Biochemistry 29*, 777−781.
12. Goodisman, J., Rehfuss, R., Ward, B., and Dabrowiak, J. C. (1992) *Biochemistry 31*, 1046−1058.
13. Goodisman, J., and Dabrowiak, J. C. (1992) *Biochemistry 31*, 1058−1064.
14. Muller, W., and Crothers, D. M. (1968) *J. Mol. Biol. 35*, 251−290.
15. Krugh, T. R. (1972) *Proc. Natl. Acad. Sci. U.S.A. 69*, 1911−1914.
16. Patel, D. J. (1974) *Biochemistry 13*, 2396−2402.
17. Krugh, T. R., Mooberry, E. S., and Chiao, Y.-C. C. (1977) *Biochemistry 16*, 740−755.
18. Brown, S. C., Mullis, K., Levenson, C., and Shafer, R. H. (1984) *Biochemistry 23*, 403−408.
19. Scott, E. V., Jones, R. L., Banville, D. L., Zon, G., Marzilli, L. G., and Wilson, W. D. (1988) *Biochemistry 27*, 915−923.
20. Scott, E. V., Zon, G., Marzilli, L. G., and Wilson, W. D. (1988) *Biochemistry 27*, 7940−7951.
21. Zhou, N., James, T. L., and Shafer, R. H. (1989) *Biochemistry 28*, 5231−5239.
22. Brown, D. R., Kurz, M., Kearns, D. R., and Hsu, V. L. (1994)-*Biochemistry 33*, 651−664.
23. Chen, F.-M. (1988) *Biochemistry 27*, 6393−6397.
24. Chen, F.-M. (1992) *Biochemistry 31*, 6223−6228.
25. Aivasashvilli, V. A, and Beabealashvilli, R. S. (1983) *FEBS Lett. 160*, 124−128.
26. Rill, R. L., Marsch, G. A., and Graves, D. E. (1989) *J. Biomol. Struct. Dyn. 7*, 591−605.
27. Snyder, J. G., Hartman, N. G., D'Estantoit, B. L., Kennard, O., Remeta, D. P., and Breslauer, K. J. (1989) *Proc. Natl. Acad. Sci. U.S.A. 86*, 3968−3972.
28. Waterloh, K., and Fox, K. R. (1992) *Biochim. Biophys. Acta 1131*, 300−306.
29. Bailey, S. A., Graves, D. E., Rill, R., and Marsch, G. (1993) *Biochemistry 32*, 5881−5887.
30. Wadkins, R. M., and Jovin, T. M. (1991) *Biochemistry 30*, 9469−9478.
31. Wadkins, R. M., Jares-Erijman, E. A., Klement, R., Rudiger, A., and Jovin, T. M. (1996) *J. Mol. Biol. 262*, 53−68.
32. Bailey, S. A., Graves, D. E., and Rill, R. (1994) *Biochemistry 33*, 11493−11500.
33. Liu, C., and Chen, F.-M. (1996) *Biochemistry 35*, 16346−16353.
34. Lian, C., Robinson, H., and Wang, A. H.-J. (1996) *J. Am. Chem. Soc. 118*, 8791−8801.
35. Sutherland, R. G., and Richards, R. I. (1994) *Am. Sci. 82*, 157−163.
36. The Huntington's Disease Collaborative Research Group (1993) *Cell 72*, 971−983.
37. LaSpada, A. R., Wilson, E. M., Lubahn, D. B., Harding, A. E., and Fischbeck, K. H. (1991) *Nature 352*, 77−99.
38. Brook, J. D., McCurrash, A. E., Harley, H. G., Buckler, A. J., Church, D., Aburatani, H., Hunter, K., Stanton, V. P., Thirion, J.-P, Hudson, T., Sohn, R., Zemelman, B., Snell, R. G., Rundle, S. A., Crow, S., Davies, J., Shelbourne, P., Buxton, J., Jones, C., Juvonen, V., Johnson, K., Harper, P. S., Shaw, D. J., and Housman, D. E. (1992) *Cell 68*, 799−808.
39. Mahadevan, M., Tsilfidis, C., Sabourin, L., Shutler, G., Amemiya, C., Jansen, G., Neville, C., Narang, M., Barcelo, J., O'Hoy, K., Leblond, S., Earle-Macdonald, J., de Jong, P. J., Wieringa, B., and Korneluk, R. G. (1992) *Science 255*, 1253−1255.
40. Chen, X., Mariappan, S. V. S., Catasti, P., Ratliff, R., Moyzis, R. K., Laayoun, A., Smith, S. S., Bradbury, E. M., and Gupta, G. (1995) *Proc. Natl. Acad. Sci. U.S.A. 92*, 5199−5203.
41. Mita, M., Yu, A., Dill, J., Kamp, T. J., Chambers, E. J., and Haworth, I. S. (1995) *Nucleic Acids Res. 23*, 1050−1059.
42. Zhu, L. M., Chou, S. H., Xu, J. D., and Reid, B. R. (1995) *Nat. Struct. Biol. 2*, 1012−1017.
43. Smith, G. K., Jie, J., Fox, G. E., and Gao, X. L. (1995) *Nucleic Acids Res. 23*, 4303−4311.
44. Mariappan, S. V. S., Garcia, A. E., and Gupta, G. (1996) *Nucleic Acids Res. 24*, 775−783.
45. Mariappan, S. V. S., Catasti, P., Chen, X., Ratliff, R., Moyzis, R. K., Bradbury, E. M., and Gupta, G. (1996) *Nucleic Acids Res. 24*, 784−792.
46. Gacy, A. M., Goellner, G., Juranic, N., Macura, S., and McMurray, C. T. (1995) *Cell 81*, 533−540.
47. Fasman, G. D., Ed. (1975) *CRC Handbook of Biochemistry and Molecular Biology*, 3rd ed., Vol. I, p 589, Chemical Rubber Company Publishing, Cleveland, OH.
48. Klotz, I. M. (1997) *Ligand−Receptor Energetics*, Wiley, New York.

BI972110X